Journal of Materials Chemistry A

COMMUNICATION

View Article Online
View Journal | View Issue

Cite this: J. Mater. Chem. A, 2016, 4, 4711

Received 26th November 2015
Accepted 26th February 2016

DOI: 10.1039/c5ta09645f

www.rsc.org/MaterialsA

Fabrication of ultrathin conductive protein-based fibrous films and their thermal sensing properties†

Xingwei Shi,[a] Er-Xia Chen,[c] Jian Zhang,[c] Hongbo Zeng[b] and Lingyun Chen*[a]

For the first time, ultrathin polypyrrole/protein fibrous films have been successfully fabricated by polymerizing pyrrole onto three-dimensional electrospun hordein network surfaces at a low temperature. The nanostructured polypyrrole is rooted on the surface of protein microfibers like "taste buds". Such modification not only eliminated the issue of protein shrinkage in the liquid medium, but also significantly improved the film's mechanical strength and wettability. The ultrathin fibrous films exhibited a "metallic" character, and could effectively respond to temperature changes, and thus have potential to be used as flexible materials for sensors and electronic devices.

Protein-based materials have attracted intensive research interest in many fields as potential substitutes for petroleum-based synthetic polymers, owing to their sustainability, biodegradability, and biocompatibility.[1–7] Additionally, the functional groups on amino acid residues allow various kinds of modifications to create new materials with advanced properties.[8–10] To date, protein-based materials used as plasticizers, packaging materials, sensors, chemical catalysts, drug-delivery systems and scaffolds have been continuously reported.[11–15]

Conducting polymers are considered as one of the stimuli-responsive polymers that display changeable and reversible conductivity by doping and undoping, and can respond to external stimuli.[16–24] For example, polyaniline with covalently bonded single-walled carbon nanotubes showed enhanced electrochromic properties in a certain range of voltage stimulation.[25] Asymmetric films formed by flash-welding polyaniline nanofiber mats demonstrated rapid reversible monolithic actuation when exposed to the camphorsulfonic acid solution.[26] Conducting polymers with low cost, lightweight, good stability, and easy preparation and handling properties are required for practical applications.

In our previous work, assembled prolamin protein fibers with zein particles as the filler were successfully prepared *via* electrospinning;[27] the addition of cellulose nanowhiskers modified with a quaternary ammonium salt can improve the mechanical properties and water resistance of hordein/zein fibers.[28] A new discovery is that by simply altering the applied voltage, the prolamin protein fibers can rapidly form flat sheets or self-rolled tubes. The release experiment indicated that the 3D porous structures could be used as carriers for controlled release of incorporated bioactive compounds.[29] It is expected that combining stimuli-responsive polymers with plant protein fibers can produce new advantageous materials. Thus, the purpose of the present work is to fabricate plant protein/conducting polymer materials by conjugation. Polypyrrole (PY) was selected as the electroactive material in this reaction system owing to its biocompatibility and good reactivity. Electrospinning is a simple and effective technology for forming micro- or nano-fiber nonwoven fabrics with a very large surface area to volume ratio and excellent pore-interconnectivity, which are particularly important for quickly starting signaling pathways. In this study, we show the feasibility to construct a nanostructured conducting polymer on the surface of protein fiber materials. The material's mechanical and thermal properties, as well as its temperature sensing capacity were investigated. Combining the protein and conducting polymer by electrospinning technology has provided an opportunity to develop new protein–polymer hybrid materials.

Fig. 1 shows the photographs of the neat hordein (HD) fibrous films and the hordein/polypyrrole (HP) fibrous films. By orientation at a rotating speed of 2000 rpm, flexible, light and almost uniaxially aligned hordein fibrous films were prepared. Using them as substrates, HP fibrous films were synthesized at −4 °C, which were also lightweight and flexible, similar to the neat hordein films. The thickness of the fibrous films could be

[a]Department of Agricultural, Food and Nutritional Science, University of Alberta, Edmonton, Canada T6G 2P5. E-mail: lingyun.chen@ualberta.ca

[b]Department of Chemical and Materials Engineering, University of Alberta, Edmonton, Alberta, T6G 2V4, Canada

[c]State Key Laboratory of Structural Chemistry, Fujian Institute of Research on the Structure of Matter, Chinese Academy of Sciences, Fuzhou, Fujian 350002, People's Republic of China

† Electronic supplementary information (ESI) available: The addition results of the HP fibrous films. See DOI: 10.1039/c5ta09645f

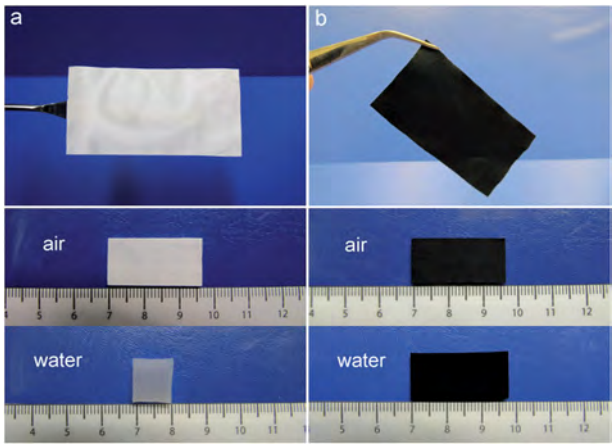

Fig. 1 Photographs of neat HD fibrous films (a) and HP fibrous films (b), and the 2.5 cm × 1.2 cm HD films and HP films placed in air and water for comparison.

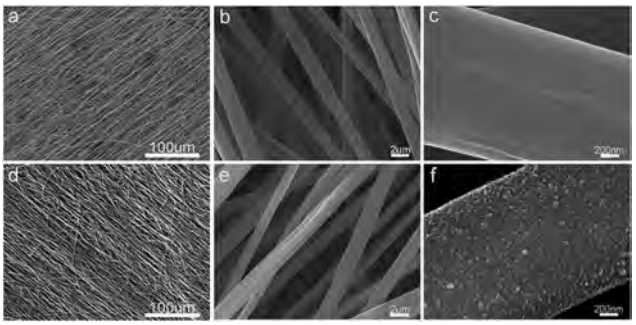

Fig. 2 SEM images of neat HD fibrous films (a–c) and HP fibrous films (d–f) with different magnifications.

mainly controlled by the electrospinning time and polymerization time. After 24 hours of polymerization reaction, the mass of the fibrous films increased by about 18 wt%. Plant protein materials normally have a poor water resistance, which can result in softening in water. Hordein fibrous films not only became soft, but also shrank when put in water, with the size decreasing from 2.5 cm × 1.2 cm to 1 cm × 1.1 cm. The remarkable super-contraction (above 50%) occurred in the direction of orientation. This behavior of the fibrous films was the same as the spider silk. When the fibrous films were wetted, the polar water molecules mainly broke the interchain hydrogen bonds of linker regions (amorphous regions) of β-sheets (the crystalline regions), and disrupted the alignment of the crystalline regions, which led to recoiling of molecular chains.[30] Additionally, it was reported that the ratio of proline in hordein was up to 21%;[31] the high amount of proline in hordein suggested a larger fraction of MaSp2 and a lower ratio of "skin".[32,33] This would allow water molecules to permeate more easily into the poorly aligned component, causing hydration and inducing a phase transition from glassy to rubbery.[34] Therefore, the neat hordein fibrous films displayed dramatic shrinkage in water. It is very interesting that the composite fibrous films did not shrink in water medium, instead, a slight expansion was observed (about 0.1 cm × 0.1 cm). It is likely that the polymerization of pyrrole on the surface of protein fibers blocked the hydration of the poorly aligned regions of hordein fibers, avoiding super-contraction as a result of the disruption of the interchain hydrogen bonds due to hydration. The slight expansion was due to the immersional wetting of water on the layer of the conducting polymer, leading to an increased area of fibrous films.

Fig. 2 shows the SEM images of the neat HD fibrous films (a–c) and HP fibrous films (d–f) with different magnifications. The neat HD fibers could be oriented to form films with arranged structure when a rotating drum with a speed of 1500 cm min^{-1} was used as the collector. The neat HD fibers displayed a smooth surface and uniform size. The diameter of the fibers can be controlled by modulating the protein concentration. It is observed in Fig. 2f that the well-defined nanostructured polypyrrole is rooted on the surface of protein microfibers like "taste buds". The diameters of the nanobuds were in the range of 10–25 nm. By controlling the reaction time and temperature, the dimensions of polypyrrole nanoparticles polymerized on the surface of protein fibers could be modulated. For example, with a long reaction time (>36 h) and high reaction temperature (>5 °C), the nanoparticles became significantly larger and less regular (Fig. S1 in the ESI†). It is interesting that at a low temperature the pyrrole monomer polymerized on the surface of the protein. Generally, polypyrrole is a black precipitate. We did not observe any black precipitate substance during the reaction, thus it is likely that no self-polymerization occurred in the solution (Fig. S2†). In order to confirm what happened on the protein surface, solid-state ^{13}C NMR spectra of neat HD films, HP fibrous films and polypyrrole powder (PY) were recorded as shown in Fig. 3. Hordein consists of a complex composition including Glu, Gln, Tyr, His, Arg, Asp, Thr, Ser, Cys and so on.[35] These amino acid units contain active side groups which can react with pyrrole monomers potentially. In the spectrum of the neat HD films, an intense and clearly distinguishable peak was observed at 173.6 ppm, due to carbonyl carbons. The resonance signals of

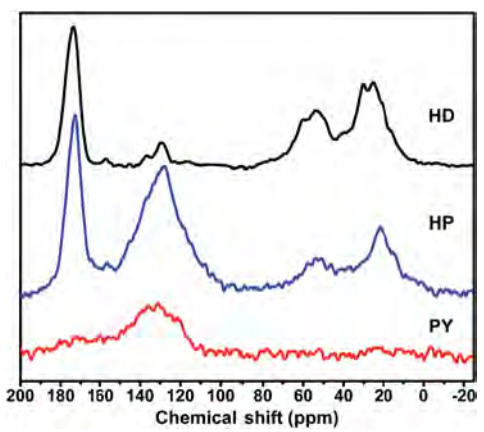

Fig. 3 Solid-state ^{13}C NMR spectra of neat HD films, HP fibrous films and polypyrrole powder (PY).

terminal carbons from Thr, Ser and Cys occurred in the region of 25 to 70 ppm, which were difficult to distinguish because of the overlap of peaks. The amino acid aromatic signals were located in the 100 to 140 ppm region.[36,37] By comparison of neat HD and HP spectra, the intensity of the peaks in the region of 25 to 70 ppm in the HP spectrum weakened and the chemical shift of the peaks changed, suggesting that the polypyrrole has been grafted on the amino acid units of hordein. Additionally, an intense and broad peak appeared in the aromatic region of the HP spectrum, indicating that the resonance signals of the aromatic rings of the polypyrrole grafted on the protein surface produced a superposition with the aromatic amino acid units of hordein. These results suggested that the peptide building blocks of the hordein protein were more reactive than pyrrole monomers themselves at a low temperature, which can be advantageous for preparing new protein-based materials. Additionally, the HD films were different with depositing or coating films on the substrate.[38–40] Based on grafting, the polypyrrole had a stronger binding force with the protein surface.

FT-IR spectra (Fig. S3†) display that the feature peaks of the composite films were almost the same as those of polypyrrole. The disappearance of the hordein peaks confirmed the growth of polypyrrole that fully covered the hordein fibrous film surface. This was consistent with the SEM image in Fig. 2f. Fig. 4 shows the schematic illustration of the polypyrrole nanobuds growing around the microfibers forming the three-dimensional fibrous film networks. Building nanoparticle, nanofiber, and nanoporous surfaces (gold, silicon, magnetic composites, polymers) is a mainstream means to achieve materials with excellent functions such as high surface-to-volume ratios, high sensitivity, and unique optical, and electrical properties.[41] The nanobuds of about 20 nm growing around the protein microfibers could provide ultrahigh active surface areas. Meanwhile, the microfibers are interconnected with each other forming a hierarchical porous structure, which is favorable for monitoring smaller changes in the environment.

In view of the fact that there may be a high temperature operating environment in practical applications, the thermogravimetric behaviors of the HD fibers, HP fibers and PY powder were also investigated in an air atmosphere, which are shown in Fig. 5. In the TGA curve of HD fibers, a small weight loss

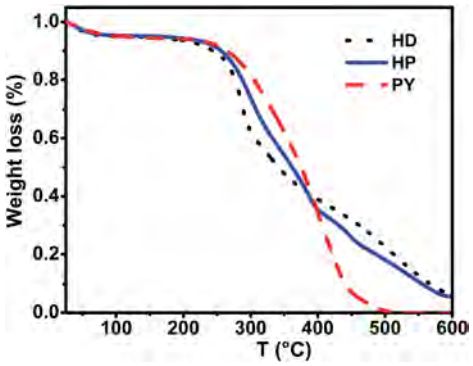

Fig. 5 DSC thermograms of neat HD films, HP fibrous films and PY powder.

occurred in the temperature ranges of 25 to 75 °C and 75 to 240 °C, respectively, due to the loss of absorbed moisture and the dehydration process. The decomposition commenced at 240 °C and significantly accelerated until 300 °C with up to 38% of weight loss, which was attributed to the degradation of the protein network. Within the temperature range of 25 to 240 °C, the HP fibers represented nearly identical curves to those of the HD fibers. However, it's noted that above 240 °C the decomposition rate of HP fibers decreased compared to HD fibers, whereas increased compared to PY powder. This result indicated that the thermal stability of the HP fibers as protein-based materials was improved. Thus, the HP fibrous films have better thermal stability which allows them to be used at a high temperature.

In order to evaluate their handling properties as flexible devices, the mechanical properties of the HP fibrous films and HD fibrous films were tested and the results are shown in Fig. 6. As expected, the tensile strength almost doubled by rooting polypyrrole on the surface of HD fibrous films, increasing from 12.6 to 21.3 MPa. The elongation (9.4%) of HP fibrous films was also significantly increased compared to that (2%) of HD fibrous films. It is worth noting that the initial modulus was decreased. Generally, the initial modulus reflects the chemical structure of the polymer as well as the magnitude of intermolecular interaction forces. The values of HP and HD fibrous films were

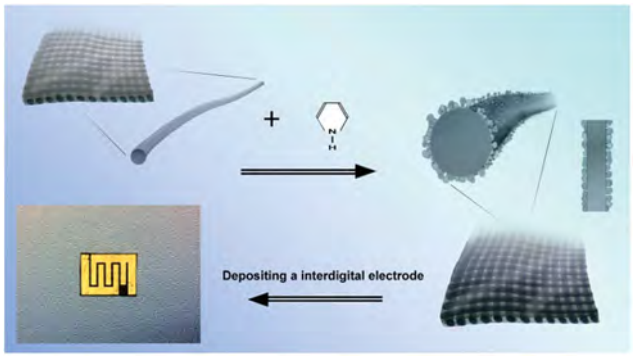

Fig. 4 Schematic illustration of the fabrication of HP fibrous films patterned with interdigitated Au electrodes.

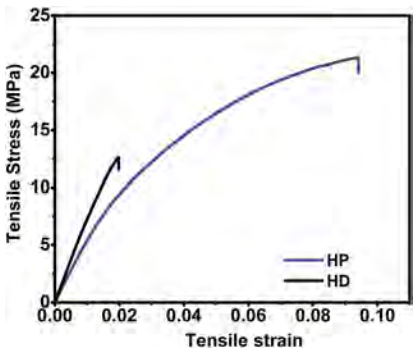

Fig. 6 Stress–strain (σ–ε) curves of neat HD fibrous films and HP fibrous films.

539 and 723 MPa, respectively. Normally the addition of the plasticizer led to an increased elongation and a reduced strength due to the reduced intermolecular interactions of the polymer matrix.[42] Whereas the addition of cellulose nanowhiskers resulted in a reduced elongation and an increased strength due to the increased intermolecular interactions of the polymer matrix and filler.[28] The modification in this research led to an increase in both strength and elongation. It is likely that the modification resulted in a strong interaction between polypyrrole and protein chains, meanwhile disrupted the degree of crystalline regions. As observed from the results of increased tensile strength and elastic compliance (reduced modulus), the HP fibrous films with improved mechanical properties will be more suitable for fabricating flexible devices.

Thermo-resistance experiments were performed to evaluate the temperature-sensing properties of the HP films when they were patterned with interdigitated Au electrodes, as shown in Fig. 4. The measurements were carried out in the operating temperature range of 30 to 150 °C. It is noteworthy that the HP fibers used in our work did not have additional doping by the dopant after washing. The resistances of the HP films would not change because of dopant volatilization during measurements. As shown in Fig. 7a, the resistance of HP films decreased dramatically with increase of temperature, and it is evident that the resistance almost had a linear relationship with temperature (Fig. 7b). The temperature coefficient (slope of the curve) resistance relative to the characteristic parameter of temperature sensing was calculated to be $-0.126\ ^{\circ}C^{-1}$. It is worth noting that the value of the temperature coefficient of HP films was almost the same order of magnitude as that of carbon nanotube materials.[43–45] The sensitivity of the HP films was calculated utilizing eqn (1). The values of sensitivity gradually increased with increase of the temperature, and were 23%, 39%, 51% and 62%, corresponding to the fixed temperature points: 60 °C, 90 °C, 120 °C and 150 °C, respectively (Fig. S4†). These results indicated that the HP films have a good response to temperature. Fig. 7c shows the continuous heating up–cooling down cycles for testing the reproducibility and reliability of HP films at 90 °C. The resistance of HP films reached the same minimum when the temperatures reached the same maximum (90 °C), and reached the same maximum at the lowest temperature (30 °C). Thereupon it was clearly observed that every time the resistance can get back to the original value if the temperature returned to the initial value, showing good recovery and stability. This result suggested that the growth of polypyrrole on the protein surface resulted in a relatively uniform nanostructure, thus thermal deformation that normally leads to irreversibility and instability could be avoided. The response

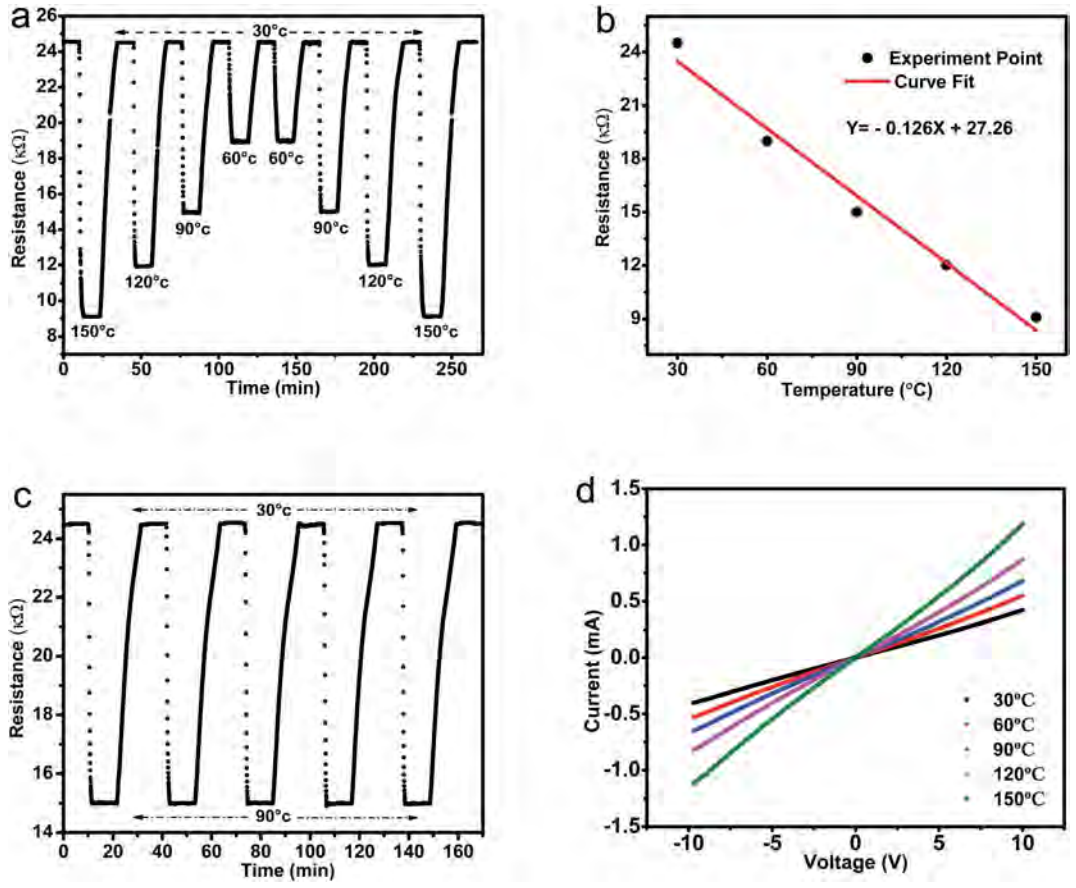

Fig. 7 Sensing performance of HP films: (a) real-time response of HP fibrous films at different temperatures; (b) calculated changes in resistance at different temperatures; (c) stability and reproducibility of HP films at 90 °C; (d) *I*–*V* characteristics of HP films at different temperatures.

time and recovery time were controlled by the thermostat controller of the equipment; no hysteresis in response rate was observed within the applied temperature change rate. The current–voltage (*I–V*) curves of HP fibers at different temperatures are shown in Fig. 7d. The resistance varied linearly with the voltage applied from −10 to 10 V, showing a "metallic" character, and indicating that the HP films had a reliable ohmic contact with the electrode.[46,47] In view of the above discussion, these ultrathin fibrous films may have a promising prospect for application as flexible materials for electronic devices and sensors.[48–54]

Conclusions

The HP fibrous films have been successfully fabricated by *in situ* polymerization at a low temperature. The nanostructured polypyrrole grew on the surface of protein microfibers like "taste buds", leading to the transformation of nonconductive protein fibers into conductive materials. The HP films displayed significantly improved mechanical properties and good thermal stability. Moreover, they showed temperature sensing properties and had reliable ohmic contact in a wide voltage range. Thus, this research has provided a new method to fabricate ultrathin conductive protein-based fibrous films as flexible materials for potential applications in electronic devices and sensors.

Experimental section

Materials

Regular barley grains (Falcon) were kindly provided by Dr James Helm, Alberta Agricultural and Rural Development, Lacombe, Alberta. The barley protein content was 13.2 wt% (dry status) as determined by combustion with a nitrogen analyzer (FP-428, Leco Corporation, St. Joseph, MI, USA) calibrated with analytical reagent grade EDTA (a factor of 6.25 was used to convert the nitrogen to protein). Hordein (total ash of 2%) was extracted using the alcohol method according to our previous work, and the protein content (dry status) was 92 wt% as determined by using the same nitrogen analyzer. Pyrrole, iron chloride, propylene glycol (PDO), and acetic acid (AC) were purchased from Sigma-Aldrich Canada Ltd. (Oakville, ON, Canada). Ethanol (EtOH) was purchased from Fisher Scientific (Markham, ON, Canada).

Preparation of HP fibrous films

0.75 g of hordein was dispersed into a mixture solvent (5 ml) with an AC/EtOH/PDO ratio of 3 : 1.5 : 0.5 by volume. The mixture was stirred vigorously with a magnetic bar for 14 hours to obtain a transparent protein solution, and then was subjected to centrifugation to remove residues at 4000 rpm for 10 min at 20 °C. The above solution was employed as a spinning dope for electrospinning by using customized digital electrospinning apparatus EC-DIG (IME Technologies, Eindhoven, Netherlands) at room temperature. The solutions were forced through a blunt needle with a diameter of 0.8 mm at a rate of 1.2 ml h^{-1}, and the applied voltage was fixed at 15.2 kV. A rotating drum with a diameter of 10 cm was chosen as the collector, and the distance between the tip and collector was set at 15 cm. A rotating speed of 2000 rpm was used to prepare uniaxially aligned electrospun fibers. To fabricate the HP fibrous films, the protein fibrous films were soaked in ethanol solution. Pyrrole and iron hydrochloric acid at a ratio of 2.5 : 1 were added into the above solution. The polymerization was carried out at 0 °C for 18 hours. The resultant HP films were washed with ethanol and deionized water, and then put on a glass plate to dry at ambient temperature.

Temperature sensitivity measurements of HP films

The measurements of the temperature sensitivity of HP films were carried out as follows: a piece of 12 × 8 × 0.021 mm^3 HP fibrous film was covered with an interdigitated mask and coated with gold by magnetron sputtering to form 0.5 mm gaps. Temperature sensing experiments were carried out on the CGS-1TP intelligent sensing analysis system with an environmental humidity of 65% and room temperature of 11 °C (Beijing Elite Tech Co., Ltd., China). The HP fibrous film electrode was put into a test box and fixed on a sheet. The heating voltage was used to heat the environment. The load resistance and the sample were connected in series and a circuit voltage was applied on them. The output voltage reflects the resistance variation of HP film electrodes. The relationship between sensitivity (S) and resistance (R) is represented by the equation:

$$S = (R_0 - R)/R_0 \times 100\% \quad (1)$$

in which, R_0 is the resistance at 30 °C, R represents the responsive resistance of the sensor electrode depending on the temperature.

Characterization

Scanning electron microscopy (SEM) measurements were carried out on a FE-SEM (FE-SEM, JAMP-9500F) by using an accelerating voltage of 20 kV. ^{13}C CP/MAS NMR spectra were recorded at room temperature using a Bruker Avance 300 MHz NMR spectrometer (Bruker Spectrospin, Karlsruhe, Germany) operating at 75.5 MHz for ^{13}C. Samples were packed in 4 mm zirconia rotors and spectra were acquired with magic-angle spinning and ^{1}H decoupling. Sample spinning for the displayed spectra was performed at 10.0 kHz though some spectra (not shown) were acquired at 8.0 kHz to verify that spectral features in the spectra shown in Fig. 3 were not due to spinning sidebands. *I–V* curves were recorded by using a Keithley 2400 Source Meter. FTIR spectra of the electrospun fibers were recorded on a Nicolet 6700 spectrophotometer (Thermo Fisher Scientific Inc., MA, USA), the samples were vacuum-dried for 24 h and then placed on an attenuated total reflectance (ATR) accessory equipped with a Gecrystal. Spectra were recorded as the average of 256 scans at 2 cm^{-1} resolution and 25 °C, using the empty accessory as blank. During measurements the accessory compartment was flushed with dry nitrogen. Thermogravimetric analysis (TGA) was carried out on TGA Q500 equipment

(TA instruments, USA) at a heating rate of 10 °C min^{-1} in an air atmosphere (40 ml min^{-1}). Tensile testing of the electrospun fibrous films was done using an Instron 5967 universal testing machine (Instron Corp., MA, USA) at a crosshead speed of 5 mm min^{-1}. Five bars with dimensions of 20 mm × 6 mm (length × width) were cut from each fabric mat along the directions of orientation. Before testing, the samples were vacuum-dried for 24 h.

Acknowledgements

The authors are grateful to the Natural Sciences and Engineering Research Council of Canada (NSERC), Alberta Crop Industry Development Fund Ltd. (ACIDF), Alberta Innovates Bio Solutions (AI Bio), and Alberta Barley Commission for financial support as well as Canada Foundation for Innovation (CFI) for equipment support. Lingyun Chen would like to thank the Natural Science and Engineering Research Council of Canada (NSERC)-Canada Research Chairs Program for its financial support.

References

1 N. Reddy and Y. Yang, *J. Appl. Polym. Sci.*, 2013, **130**, 729–738.
2 L. S. Witus and M. B. Francis, *Acc. Chem. Res.*, 2011, **44**, 774–783.
3 A. J. Poole, J. S. Church and M. G. Huson, *Biomacromolecules*, 2009, **10**, 1–8.
4 F. Song, D. Tang, X. Wang and Y. Wang, *Biomacromolecules*, 2011, **12**, 3369–3380.
5 R. Zhu, H. Liu and J. Zhang, *Ind. Eng. Chem. Res.*, 2012, **51**, 7786–7792.
6 F. Chen and J. Zhang, *ACS Appl. Mater. Interfaces*, 2010, **2**, 3324–3332.
7 S. Sinha-Ray, Y. Zhang, A. L. Yarin, S. C. Davis and B. Pourdeyhimi, *Biomacromolecules*, 2011, **12**, 2357–2363.
8 M. Geisler, S. Xiao, E. M. Puchner, F. Grater and T. Hugel, *J. Am. Chem. Soc.*, 2010, **132**, 17277–17281.
9 N. P. King, W. Sheffler, M. R. Sawaya, B. S. Vollmar, J. P. Sumida, I. André, T. Gonen, T. O. Yeates and D. Baker, *Science*, 2012, **336**, 1171–1174.
10 C. S. Thomas, M. J. Glassman and B. D. Olsen, *ACS Nano*, 2011, **5**, 5697–5707.
11 J. N. Renner, K. M. Cherry, R. S. C. Su and J. C. Liu, *Biomacromolecules*, 2012, **13**, 3678–3685.
12 A. M. Jonker, D. W. P. M. Lowik and J. C. M. Hest, *Chem. Mater.*, 2012, **24**, 759–773.
13 J. F. Almine, D. V. Bax, S. M. Mithieux, L. Nivison-Smith, J. Rnjak, A. Waterhouse, S. G. Wise and A. S. Weiss, *Chem. Soc. Rev.*, 2010, **39**, 3371–3379.
14 R. de la Rica and H. Matsui, *Chem. Soc. Rev.*, 2010, **39**, 3499–3509.
15 R. H. Farahi, A. Passian, L. Tetard and T. Thundat, *ACS Nano*, 2012, **6**, 4548–4556.
16 H. Bai and G. Shi, *Sensors*, 2007, **7**, 267–307.
17 O. S. Kwon, S. J. Park, J. S. Lee, E. Park, T. Kim, H. W. Park, S. A. You, H. Yoon and J. Jang, *Nano Lett.*, 2012, **12**, 2797–2802.
18 J. Janata and M. Josowicz, *Nat. Mater.*, 2003, **2**, 19–24.
19 C. Chuang, H. Wu, Y. Huang and C. Chen, *Biosens. Bioelectron.*, 2013, **48**, 158–164.
20 X. Shi, L. Zhang, J. Cai, G. Cheng, H. Zhang, J. Li and X. Wang, *Macromolecules*, 2011, **44**, 4565–4568.
21 X. Shi, A. Lu, J. Cai, L. Zhang, H. Zhang, J. Li and X. Wang, *Biomacromolecules*, 2012, **13**, 2370–2378.
22 X. Shi, Y. Hu, L. Zhang, H. Zhang, J. Li and X. Wang, *Soft Matter*, 2013, **9**, 10129–10134.
23 X. Shi, Y. Hu, F. Fu, J. Zhou, Y. Wang, L. Chen, H. Zhang, J. Li, X. Wang and L. Zhang, *J. Mater. Chem. A*, 2014, **2**, 7669–7673.
24 A. G. MacDiarmid, *Synth. Met.*, 2002, **125**, 11–22.
25 S. Xiong, J. Wei, P. Jia, L. Yang, J. Ma and X. Lu, *ACS Appl. Mater. Interfaces*, 2011, **3**, 782–788.
26 C. O. Baker, B. Shedd, P. C. Innis, P. G. Whitten, G. M. Spinks, G. G. Wallace and R. B. Kaner, *Adv. Mater.*, 2008, **20**, 155–158.
27 Y. Wang and L. Chen, *J. Mater. Chem.*, 2012, **22**, 21592–21601.
28 Y. Wang and L. Chen, *ACS Appl. Mater. Interfaces*, 2014, **6**, 1709–1718.
29 Y. Wang, J. Yang and L. Chen, *ACS Appl. Mater. Interfaces*, 2015, **7**, 13422–13430.
30 Z. Yang, O. Liivak, A. Seidel, G. LaVerde, D. B. Zax and L. W. Jelinski, *J. Am. Chem. Soc.*, 2000, **122**, 9019–9025.
31 Y. Wang and L. Chen, *Macromol. Mater. Eng.*, 2012, **297**, 902–913.
32 R. Beckwitt and S. Arcidiacono, *J. Biol. Chem.*, 1994, **269**, 6661–6663.
33 A. Sponner, E. Unger, F. Grosse and W. Klaus, *Nat. Mater.*, 2005, **4**, 772–775.
34 Y. Liu, A. Sponner, D. Porter and F. Vollrath, *Biomacromolecules*, 2008, **9**, 116–121.
35 Y. Wang and L. Chen, *Macromol. Mater. Eng.*, 2012, **297**, 902–913.
36 M. E. Augustine and I. C. Baianu, *J. Cereal Sci.*, 1986, **4**, 371.
37 D. Sharma and K. Rajarathnam, *J. Biomol. NMR*, 2000, **18**, 165–171.
38 P. C. Wang, R. E. Lakis and A. G. MacDiarmid, *Thin Solid Films*, 2008, **516**, 2341–2345.
39 P. C. Wang, L. H. Liu, D. A. Mengistie, K. H. Li, B. J. Wen, T. S. Liu and C. W. Chu, *Displays*, 2013, **34**, 301–314.
40 J. Choi, I. Lee and S. Y. Lee, *Langmuir*, 2009, **25**, 11495–11502.
41 R. C. Webb, A. P. Bonifas, A. Behnaz, Y. Zhang, K. Yu, H. Cheng and J. A. Rogers, *Nat. Mater.*, 2013, **12**, 938–944.
42 J. Zhang, P. Mungara and J. Jane, *Polymer*, 2001, **42**, 2569–2578.
43 P. S. Dorozhkin, S. V. Tovstonog, D. Golberg, J. Zhan, Y. Ishikawa, M. Shiozawa, H. Nakanishi, K. Nakata and Y. Bando, *Small*, 2005, **1**(11), 1088–1093.
44 C. Y. Kuo, C. L. Chan, C. Gau, C. Liu, S. H. Shiau and J. H. Ting, *Nanotechnology*, 2007, **6**, 63–69.

45 A. D. Bartolomeo, M. Sarno, F. Giubileo, C. Altavilla, L. Iemmo, S. Piano, F. Bobba, M. Longobardi, A. Scarfato, D. Sannino, A. M. Cucolo and P. Ciambelli, *J. Appl. Phys.*, 2009, **105**, 064518.
46 B. Z. Cvetkovi, J. Puigmartí-Luis, D. Schaffhauser, T. Ryll, S. Schmid and P. S. Dittrich, *ACS Nano*, 2013, **7**, 183–190.
47 L. Mai, L. Xu, Q. Gao, C. Han, B. Hu and Y. Pi, *Nano Lett.*, 2010, **10**, 2604–2608.
48 H. Liu, M. Li, O. Voznyy, L. Hu, Q. Fu, D. Zhou, Z. Xia, E. H. Sargent and J. Tang, *Adv. Mater.*, 2014, **26**, 2718–2724.
49 M. Melnykowycz, B. Koll, D. Scharf and F. Clemens, *Sensors*, 2014, **14**, 1278–1294.
50 S. Ammu, V. Dua, S. R. Agnihotra, S. P. Surwade, A. Phulgirkar, S. Patel and S. K. Manohar, *J. Am. Chem. Soc.*, 2012, **134**, 4553–4556.
51 W. Yuan and G. Shi, *J. Mater. Chem. A*, 2013, **1**, 10078–10091.
52 S. Gong, W. Schwalb, Y. Wang, Y. Chen, Y. Tang, J. Si, B. Shirinzadeh and W. Cheng, *Nat. Commun.*, 2014, **5**, 3132–3139.
53 H. Uehara, M. Kakiage, M. Sekiya, D. Sakuma, T. Yamonobe, N. Takano, A. Barraud, E. Meurville and P. Ryser, *ACS Nano*, 2009, 924–932.
54 M. C. McAlpine, H. Ahmad, D. Wang and J. R. Heath, *Nat. Mater.*, 2007, 379–384.